Cell

L3MBTL1, a Histone-Methylation-Dependent Chromatin Lock

Patrick Trojer,[1,2,3,7] Guohong Li,[1,2,3,7] Robert J. Sims, III,[2,3,7] Alejandro Vaquero,[1,2,6] Nagesh Kalakonda,[4] Piernicola Boccuni,[4] Donghoon Lee,[2] Hediye Erdjument-Bromage,[5] Paul Tempst,[5] Stephen D. Nimer,[4] Yuh-Hwa Wang,[2] and Danny Reinberg[1,2,3,*]
[1] Howard Hughes Medical Institute
[2] Department of Biochemistry, Division of Nucleic Acids Enzymology, Robert Wood Johnson Medical School
University of Medicine and Dentistry of New Jersey, 683 Hoes Lane, Piscataway, NJ 08854, USA
[3] Department of Biochemistry, New York University Medical School, 522 First Avenue, New York, NY 10016, USA
[4] Laboratory of Molecular Aspects of Hematopoiesis
[5] Protein Center and Molecular Biology Program
Sloan Kettering Institute for Cancer Research, New York, NY 10021, USA
[6] Present address: ICREA and IBMB, CSIC/IRB, Parc Cientific de Barcelona, Josep Samitier 1-5, 08028 Barcelona, Spain.
[7] These authors contributed equally to this work.
*Correspondence: reinbd01@med.nyu.edu
DOI 10.1016/j.cell.2007.03.048

SUMMARY

Distinct histone lysine methylation marks are involved in transcriptional repression linked to the formation and maintenance of facultative heterochromatin, although the underlying mechanisms remain unclear. We demonstrate that the *m*alignant-*b*rain-*t*umor (MBT) protein L3MBTL1 is in a complex with core histones, histone H1b, HP1γ, and Rb. The MBT domain is structurally related to protein domains that directly bind methylated histone residues. Consistent with this, we found that the L3MBTL1 MBT domains compact nucleosomal arrays dependent on mono- and dimethylation of histone H4 lysine 20 and of histone H1b lysine 26. The MBT domains bind at least two nucleosomes simultaneously, linking repression of transcription to recognition of different histone marks by L3MBTL1. Consistently, L3MBTL1 was found to negatively regulate the expression of a subset of genes regulated by E2F, a factor that interacts with Rb.

INTRODUCTION

Chromatin, the organized assemblage of histones and genomic DNA, is critical to the proper regulation of cellular processes associated with DNA metabolism, including transcription. Covalent histone modifications, chromatin remodeling, and histone exchange contribute to dynamic chromatin structure changes that impact transcriptional regulation. Silencing of gene expression is partially achieved by transient or stable condensation of the chromatin structure (facultative or constitutive heterochromatin, respectively), which renders DNA inaccessible to the transcription machinery. Histone lysine methyltransferases (HKMTs) that target H3K9, H3K27, and H4K20 are important for the establishment and maintenance of heterochromatin, but the underlying mechanisms remain elusive (Sims et al., 2003). These histone lysine methylation marks serve as recognition sites for chromatin-binding proteins ("readers"), which may directly compact chromatin structure or recruit other chromatin-effector proteins.

The linker histone H1 is thought to be an important mediator of higher-order chromatin structure (Bednar et al., 1995; Sato et al., 1999). Recently, lysine 26 was identified as a target for acetylation and methylation within the histone H1 variant H1b/H1.4/H1^{s}-4 (H1bK26; Kuzmichev et al., 2004; Vaquero et al., 2004); however, the biological significance remains unknown.

Histone modifications such as H3K27 methylation, H3K9 dimethylation (H3K9me2), and H4K20 monomethylation (H4K20me1) are commonly found in facultative heterochromatin (Sims et al., 2003). Methylated H3K27 is recognized by Polycomb, a component of Polycomb repressive complex 1 (PRC1). However, recently PRC1 was shown to compact nucleosomal arrays in vitro independent of H3K27 methylation or histone tails (Francis et al., 2004). H3K9 di- and trimethylation are directly recognized by HP1 (Bannister et al., 2001; Jacobs et al., 2001). HP1 localizes to facultative and constitutive heterochromatin, associates with the H3K9-specific HKMT SUV39H1 (Schotta et al., 2002), and can mediate the spreading of H3K9 methylation by oligomerization (Hall et al., 2002). HP1 binding to chromatin is highly dynamic and in some instances is independent of H3K9 methylation (Meehan et al., 2003). Of the three mammalian HP1 isoforms, HP1α and -β are predominantly associated with constitutive heterochromatin, and HP1γ is found in euchromatin and facultative heterochromatin (Minc

et al., 2000). HP1 also binds to recombinant nucleosomes, DNA, and RNA (Maison et al., 2002; Zhao et al., 2000). In contrast, the functional significance of H4K20me1 mediated by PR-SET7 (Nishioka et al., 2002) remains far less understood.

L3MBTL1 is of great interest in this context. The *m*alignant-*b*rain-*t*umor (MBT) domain was first described in the *Drosophila* tumor-suppressor protein L(3)mbt (Wismar et al., 1995). Recessive or temperature sensitive mutations of the *D-l(3)mbt* gene cause malignant transformation in the larval brain. Various mutations were found to impair synchronous cell division and mitotic progression in the early stages of *Drosophila* embryonic development (Yohn et al., 2003). Human L3MBTL1 is a known transcriptional repressor (Boccuni et al., 2003), which requires its three MBT domains for silencing. A screen for novel chromatin-binding domains revealed that the second and third MBT domain of L3MBTL1 bound to monomethyl H3K4 and dimethyl H4K20 (Kim et al., 2006). Another MBT family member, *Drosophila* Sfmbt, was recently shown to bind to mono- and dimethylated H3K9 and to dimethylated H4K20 peptides (Klymenko et al., 2006). Yet, the functional implications of this binding event are not known.

Using sucrose gradient sedimentation to reconstitute L3MBTL1-histone complexes followed by electron microscopy (EM) analyses, we demonstrate that L3MBTL1 compacts nucleosomal arrays in a manner that requires specific posttranslational modifications within core and/or linker histones. The second MBT domain of L3MBTL1 exclusively recognizes the mono- and dimethyl versions of both H4K20 and H1bK26, respectively. Our studies identify a novel mechanism for the readout of multiple lysine methylation marks within histones H1b, H3, and H4 via a singular complex of L3MBTL1 and HP1γ and suggest that a combinatorial pattern of histone modifications results in a direct functional outcome—specifically, chromatin condensation at Rb-regulated genes.

RESULTS

L3MBTL1 Associates with Core Histones, Histone H1 and HP1γ

The human L3MBTL1 (isoform 1) protein comprises 772 amino acids ($\sim$100 kDa) and contains three identifiable domains (Figure 1A). To tackle the mechanistic aspects of L3MBTL1-mediated transcriptional repression (Boccuni et al., 2003), we generated a 293 cell line that constitutively expresses full-length L3MBTL1 containing a FLAG epitope at its C terminus (L3MBTL1-F). L3MBTL1-F and its associated proteins were identified after affinity purification from nuclear extracts (Figure 1A and see below). A cell line stably transfected with empty vector (mock) served as control. Silver staining revealed a number of polypeptides that specifically associate with L3MBTL1-F. These polypeptides were found to be core histones, histone H1b, HP1γ, and the Retinoblastoma protein (Rb; Figure 1A).

The MBT Domains of L3MBTL1 Compact Chromatin in a Core-Histone-Modification-Dependent Manner

To determine the functional relevance of core histones present in a complex with L3MBTL1, we first investigated whether their modifications contributed to this interaction. Nucleosomal arrays were reconstituted with bacterially expressed histones (recombinant chromatin) or histones purified from HeLa cells (native chromatin) and then incubated with a recombinant protein encompassing the three MBT repeats of L3MBTL1 fused to GST (GST-3MBT; Figure 1A). Initially the association of GST-3MBT with histones was analyzed by sucrose gradient sedimentation followed by EM. Fractions derived from the sucrose gradients were analyzed by western blot using anti-3MBT antibodies (Figure 1B). The GST-3MBT protein migrated near top of the gradient but shifted toward the bottom upon the addition of native chromatin templates (Figure 1B). Importantly, this shift was not observed in the presence of recombinant chromatin. A similar profile was observed upon inspection of the sedimentation profile of nucleosomal DNA (Figure 1C).

The peak fractions from the sucrose gradient (see Figure 1C) were analyzed by EM to explore any visible changes to the chromatin template upon GST-3MBT binding. In the absence of GST-3MBT, recombinant and native nucleosomal arrays displayed a typical ''beads on a string'' configuration (11 nm fiber), confirming a proper chromatin reconstitution in both cases (Figure 1D). The recombinant chromatin was treated with the HAT-p300 and acetyl coenzyme A to allow acetylation and the establishment of 11 nm fibers (Loyola et al., 2001). Since the native and recombinant chromatin both contained acetylated residues (data not shown), we concluded that acetylation per se does not impair binding of MBT to chromatin (see Experimental Procedures; Figures 1D, 2B, 5B, and 5C; Table 1).

Strikingly, the native chromatin particles became highly compacted upon GST-3MBT addition (Figure 1D; magnified image of one compacted particle in upper right panel). Quantification of the observed structural changes revealed that $\sim$70% of the molecules became fully compacted by GST-3MBT (data not shown). In contrast, the recombinant nucleosome arrays were unaffected and remained in the 11 nm fiber configuration. Addition of GST protein alone was ineffectual (data not shown). L3MBTL1 can homodimerize via its SPM domain (Boccuni et al., 2003), and GST-3MBT can do so through the GST domain. To analyze if dimerization was a factor, we produced a hexahistidine-tagged 3MBT protein (His-3MBT). Superdex-200 size-exclusion chromatography verified that His-3MBT was monomeric (Figure S1). The monomeric His-3MBT polypeptide also compacts native chromatin but not recombinant chromatin (Figure S2). We conclude that the 3MBT not only binds modified core histones in nucleosome arrays but also compacts these arrays in a strictly histone-modification-dependent manner.

We next tested which, if any, of the six major histone-methylation sites on core histones is/are responsible for

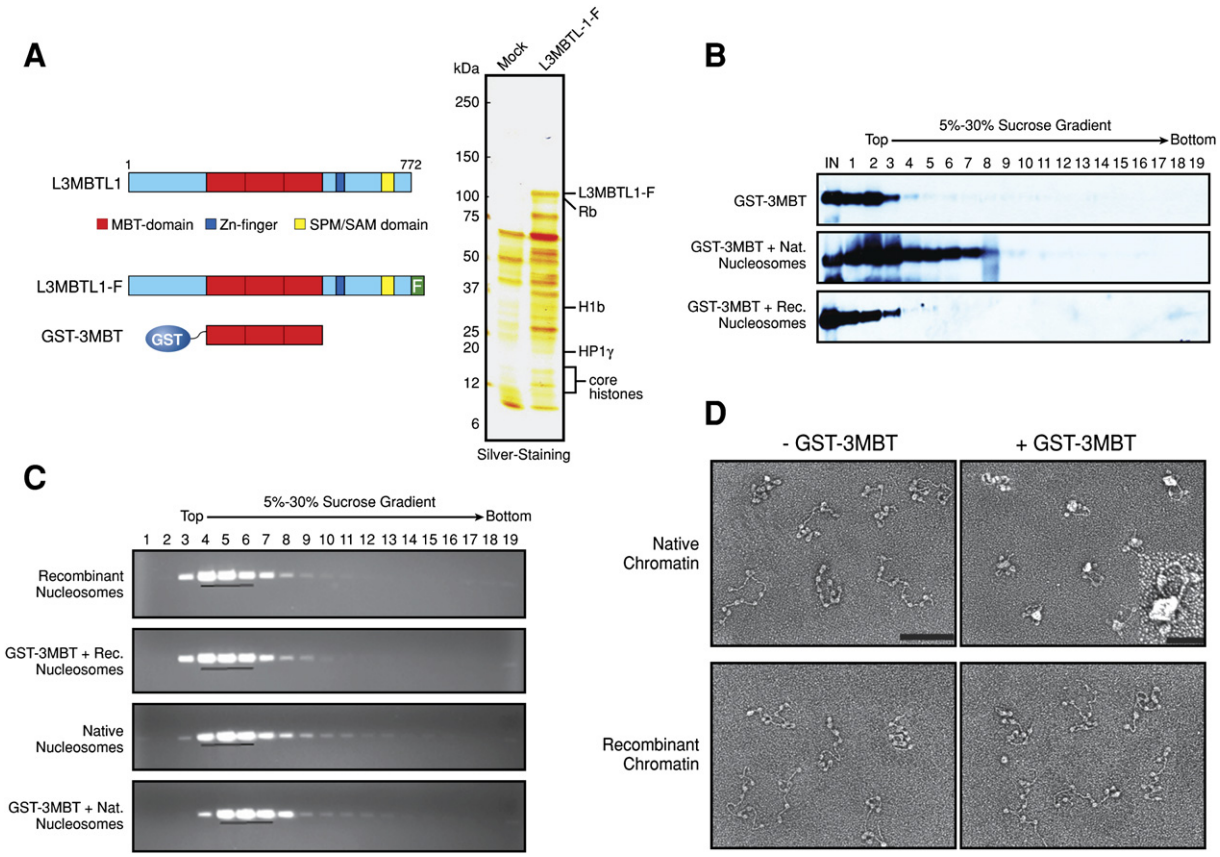

Figure 1. Purification of L3MBTL1-Associated Proteins and Chromatin Compaction by L3MBTL1 in a Histone-Modification-Dependent Manner

(A) Left panel: Schematic of the L3MBTL1 domain organization and constructs used for eukaryotic expression (L3MBTL1-F) or prokaryotic expression (GST-3MBT). Right panel: Silver staining of proteins purified from 293 cells expressing L3MBTL1-F or empty vector (Mock) using anti-FLAG (M2) agarose. Proteins identified by mass spectrometry or western blot are indicated.

(B) Western blot of sucrose gradient fractions containing GST-3MBT or recombinant or native oligonucleosomes incubated with GST-3MBT using anti-3MBT antibodies.

(C) Sucrose gradient fractions as in (B) analyzed by agarose gel electrophoresis and ethidium bromide staining.

(D) Sucrose gradient peak fractions as determined in (C) subjected to electron microscopy (EM) analysis. Scale bar is 100 nm, and bar in the insert is 25 nm.

L3MBTL1 binding and compaction using, initially, peptide-affinity binding assays. GST-3MBT protein bound specifically to H4K20me1/2 but not to unmodified H4K20 or H4K20me3 (Figure 2A). GST-3MBT did not bind to methylated H3K4, H3K9, and H3K27 peptides, but HP1γ bound to H3K9me2 (Figure S3), and hCHD1 bound to H3K4me (data not shown). Collectively these results establish that in peptide pull-down assays, GST-3MBT binds specifically to mono- and dimethylated H4K20.

To address the chromatin-compaction potential of GST-3MBT in the context of H4K20me1 and nucleosome arrays, we employed PR-SET7, the enzyme that catalyzes the addition of a single methyl group to H4K20 (Nishioka et al., 2002). PR-SET7 was used to methylate recombinant nucleosomal arrays in vitro, and subsequent addition of GST-3MBT protein was analyzed by sucrose gradient sedimentation. Only chromatin that was premethylated (+S-adenosyl-methionine [SAM]) induced a migration shift upon GST-3MBT addition (data not shown). Using EM, we observed a number of compacted chromatin particles as a function of GST-3MBT binding (Figure 2B; Table 1). We repeated these experiments using monomeric His-3MBT protein and observed a similar outcome, chromatin compaction (Table 1). This compaction was dependent on the presence of SAM, confirming that L3MBTL1 could bind and compact nucleosome arrays containing H4K20me1.

L3MBTL1 Interacts with HP1γ

We next explored the basis of HP1γ association with L3MBTL1. To score for specificity, we compared the proteins present in the L3MBTL1-F fraction to those associated with its two close homologs, L3MBTL2-F and

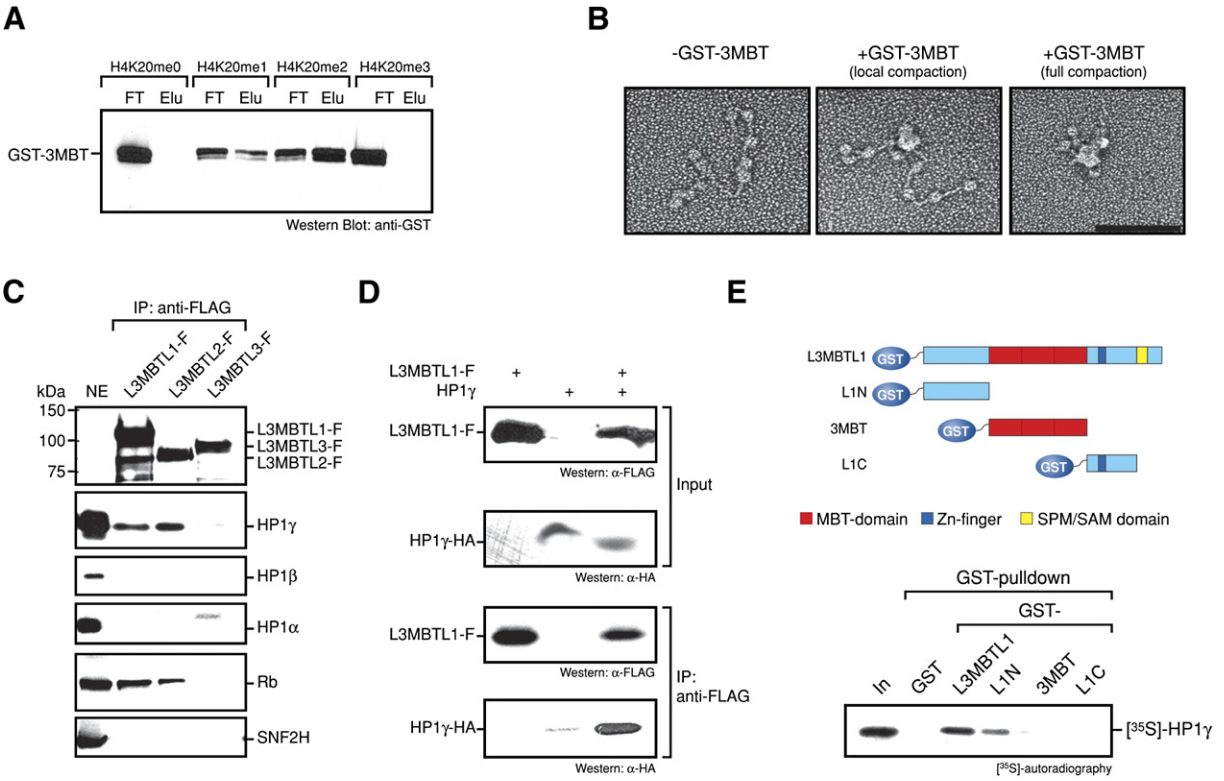

Figure 2. H4K20 Monomethylation Is Sufficient to Recruit L3MBTL1 with Resultant Chromatin Compaction

(A) Immunoblotting (anti-GST antibody) of peptide affinity chromatography fractions (flow-through [FT]); bound fraction [Elu]) using crosslinked histone H4 peptides, either unmodified, mono-, di-, or tri-methylated at K20 (H4K20me1/2/3) and GST-3MBT.

(B) EM analysis of sucrose gradient peak fractions performed similarly to the experiment shown in Figure 1C using recombinant reconstituted nucleosomal arrays monomethylated at H4K20 with PR-SET7. Scale bar is 100 nm.

(C) Western blot of polypeptides associated with L3MBTL1-F, L3MBTL2-F, and L3MBTL3-F using the antibodies indicated. Nuclear extract (NE) was used as input, and anti-SNF2H antibody was used as negative control.

(D) 293 cells were transiently transfected with expression vectors encoding HP1γ-HA and L3MBTL1-F. Extracts were subjected to anti-FLAG (M2) agarose, and bound proteins were monitored by immunoblot with anti-FLAG and anti-HA antibodies.

(E) Top panel: Representation indicating the sizes of recombinant L3MBTL1 fragments used for GST pull-downs. Bottom panel: Recombinant GST and GST-L3MBTL1 fragments and in-vitro-translated [^{35}S]-labeled HP1γ used for GST pull-downs. Precipitated proteins were monitored by autoradiography.

L3MBTL3-F. We analyzed the association of HP1 using specific antibodies that discriminate between the three mammalian HP1 isoforms in western blot. Biochemical fractionation of cellular extracts revealed that HP1γ is more abundant in nuclear extracts compared to the α or β isoforms (Figure S4A; Nielsen et al., 2001). HP1α and -β were not present, but HP1γ was detected in the L3MBTL1 and L3MBTL2 affinity-purified fractions (Figure 2C), a result consistent with previous findings (Ogawa et al., 2002). This interaction is specific, as the L3MBTL3-F affinity-purified fraction was devoid of HP1γ. Using two antibodies from different sources, we also detected the human Rb protein within the affinity-purified L3MBTL1 and L3MBTL2 samples, but not in the case of L3MBTL3 (Figure 3A and data not shown).

Anti-FLAG-immunoprecipitation of cotransfected cells demonstrates that HA-tagged HP1γ coimmunoprecipitated only in the presence of L3MBTL1-F (Figure 2D). As well, in-vitro-translated full-length L3MBTL1 precipitated with GST-HP1γ (Figure S4B). The N terminus of L3MBTL1 interacted with HP1γ (Figure 2E), but since these studies were performed using protein translated in vitro, we cannot conclude that the interaction is direct; however, we can rule out an indirect association mediated through core histones as these interact exclusively with the MBT domains and not the N-terminal region of L3MBTL1 (data not shown).

L3MBTL1 Directly and Specifically Binds to H1bK26me1/2

Given the presence of H1b in the affinity-purified preparation of L3MBTL1-F, we analyzed for their interaction in vivo using cotransfection experiments in 293 cells with either L3MBTL1-F or L3MBTL2-F and HA-tagged histone H1b/H1.4 (H1b-HA). H1b coprecipitated with L3MBTL1-F but not with L3MBTL2-F using anti-FLAG antibodies

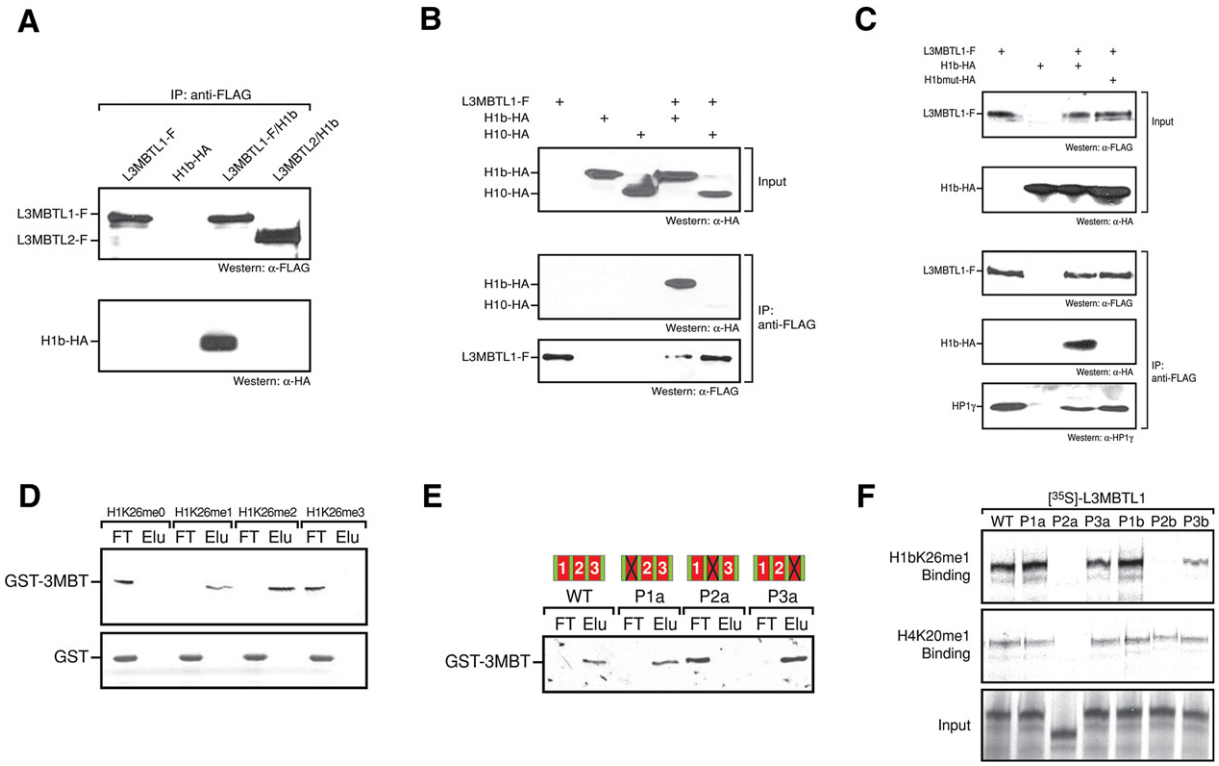

Figure 3. L3MBTL1 Interacts with H1b In Vivo and In Vitro

(A) IP performed on extracts from 293 cells cotransfected with expression vectors encoding H1b-HA and either L3MBTL1-F or L3MBTL2-F.

(B) As in (A) but with L3MBTL1-F and either H1b-HA or H1.0-HA.

(C) As in (A) but with L3MBTL1-F and H1b-HA, either wild-type or with K26A point mutation.

(D) Peptides comprising amino acids 20–37 of histone H1b either unmodified, mono-, di-, or tri-methylated at K26 (H1K26me0/1/2/3) immobilized to sulfolink resin and incubated with recombinant GST or GST-3MBT. Bound (Elu) and unbound (FT) proteins were monitored by silver staining.

(E) Silver stain of interactions between immobilized H1b-K26me2 peptides and recombinant GST-3MBT either wild-type or with point mutations P1a, P2a, and P3a in the first, second, and third MBT domain, respectively.

(F) Autoradiography of interactions between immobilized H1b-K26me1 or H4-K20me1 peptides and full-length in-vitro-translated [^{35}S]-labeled L3MBTL1, either wild-type or with P1a or P1b, P2a or P2b, or P3a or P3b point mutants (see Supplemental Data for details) in the first, second, and third MBT domain, respectively.

(Figure 3A). A similar result was obtained in reciprocal immunoprecipitation assays (Figure S5). We analyzed if L3MBTL1-F interacts with additional H1 isotypes. Cotransfection experiments with the histone variants H1o/H1.0 were performed. Histone H1b, but not H1o, interacted with L3MBTL1-F (Figure 3B). Histone H1b can be methylated at lysine 26 (H1bK26me; Kuzmichev et al., 2005), and this residue is not present in H1o. Similar to the H1o case, a mutant form of H1b containing a substitution of lysine-26 to alanine (H1b-K26A; Kuzmichev et al., 2004) did not immunoprecipitate with L3MBTL1-F (Figure 3C).

Since all HP1 isoforms recognize and bind dimethylated H1b-K26 (Daujat et al., 2005), the observed interaction of HP1γ with L3MBTL1-F (Figure 1A) could be mediated through its interaction with H1. However, the amount of endogenous HP1γ in the anti-FLAG immunoprecipitates was relatively similar regardless of whether H1b was coprecipitated or not (Figure 3C). Collectively, our data indicate that L3MBTL1 is associated with HP1γ, nucleosomes containing H4K20me1 and H1b and that the K26 residue of H1b is important for its interaction with L3MBTL1. Moreover, the presence of Rb in the L3MBTL1 complex suggests a means of directing L3MBTL1 to target genes.

To determine if the interaction between L3MBTL1 and H1b is direct and if methylation of K26 is required, we initially used peptide-affinity chromatography. Affinity columns were generated with H1b peptides comprising residues 20–37 in which K26 was un-, mono-, di-, or trimethylated and incubated with GST-3MBT. GST-3MBT binds to the mono- and dimethylated peptides but not to the unmethylated or trimethylated versions (Figure 3D). We next tested GST-3MBT proteins containing single amino acid substitutions in each of the MBT domains (P1a, P2a, and P3a; Figure S6) at residues which are predicted to be important for binding (Wang et al., 2003). The P1a and P3a mutant proteins bound, but not the P2a mutant (Figure 3E). We expanded the binding studies and

found that full-length in-vitro-translated L3MBTL1 protein bound mono- and dimethylated H1 peptides exclusively (Figure 3F and data not shown). Notably, the in-vitro-translated full-length P2a mutant protein (but not the recombinant GST-3MBT P2a mutant) migrates faster in SDS-PAGE; the reason for this is not known. In this experiment, we used a different set of mutant proteins, each with a single amino acid substitution (P1b, P2b, and P3b; Figure S6) and again observed that only mutation in the second MBT domain abolished interaction (Figure 3F). A point mutation in the third pocket led to decreased binding, suggesting that both pockets might cooperate in binding methylated histone lysines. Interestingly, the P2a mutation also abolished binding to H4K20me1, but the P2b mutant was unaffected (Figure 3F). These data suggest that both H1K26 and H4K20 are bound via the second MBT domain; however, a different set of residues seems to be involved in H1K26me versus H4K20me binding.

To validate these findings, interaction experiments were performed using GST-3MBT and bacterially expressed full-length histone H1b containing an HA tag. As expected, bacterially produced (unmodified) H1b did not interact with GST-3MBT (data not shown). It was shown previously that G9a can dimethylate H3K9 and histone H1 in vitro (Tachibana et al., 2001). When G9a was used to methylate wild-type H1b and mutant H1bK26A proteins, GST-3MBT bound to G9a-methylated H1b but not to the methylation-deficient H1bK26A mutant. Kinetic and substrate-specificity studies determined that G9a is capable of mono- and dimethylation in a time-dependent manner (Patnaik et al., 2004). Indeed, using an antibody that specifically recognizes H1bK26me2, we confirmed that G9a dimethylates H1K26 and that H1b dimethylated at K26 binds to GST-3MBT (Figure 4A).

Of note, the H1b sequence containing lysine-26 is similar to the sequences surrounding H3K9 and H3K27 (ARKS). However, we did not observe binding of GST-3MBT to the H3K9 and H3K27 peptides, regardless of their methylation status (Figure S3). Collectively, our results show that the MBT repeats of L3MBTL1 directly interact with mono- or dimethylated histone H1bK26.

MBT Domains Compact Chromatin in an H1bK26me1/2-Dependent Manner

Our results show that L3MBTL1 interacts with H1bK26me1/2. Histone H1 is implicated in the formation of higher-order chromatin and can function on its own in compaction of chromatin templates in vitro (Bednar et al., 1995). We next investigated the role of the MBT domains in conjunction with H1 in this process. Recombinant or native histone H1b was incorporated onto spaced nucleosomes that were confirmed as such by MNase digestion (data not shown). Chromatin compaction in the presence or absence of GST-3MBT was analyzed by sucrose gradient sedimentation followed by EM as described above. Under the conditions used whereby recombinant core histones are acetylated with p300, a preparation of human histone H1 by itself did not efficiently compact the chromatin templates (Figure 4B, left panel). Remarkably, and in contrast to its inability to do so alone, GST-3MBT was observed to compact recombinant nucleosome arrays upon the incorporation of native, but not recombinant, H1 (Figure 4B, right panel; Table 1; data not shown).

The native H1 preparation that successfully gave rise to compacted molecules in a GST-3MBT-dependent manner is presumably comprised of different H1 variants with multiple posttranslational modifications. Thus, the compaction assay was repeated using recombinant H1b that was methylated by G9a before incorporation into nucleosomes. GST-3MBT compacted a significant number of these particles (Figure 4C; Table 1). Two types of molecules were generally observed. In one case, the molecules contained a loop, the other type of molecules did not loop, but the array appeared to be compacted (Figure 4C). Regardless, the increase in looping and/or compaction was dependent on H1b methylation (Table 1). These results provided further evidence that the MBT domains bind H1K26me1/2 in the context of nucleosome arrays and, more importantly, suggest that L3MBTL1 binding to H1bK26me1/2 yields a distinct functional outcome, the compaction of chromatin fibers.

The MBT Domains of L3MBTL1 Can Bind Two Nucleosomes Simultaneously

The specificity of binding of the three MBT domains to two different methylated histone lysine residues, together with the mutational analyses presented above (Figure 3), raised an interesting question: Can a single 3MBT domain bind simultaneously to two different histone lysine methylation marks? To address this question we used the monomeric His-3MBT protein, which was incubated with various histone peptides. The peptide-protein complexes were then loaded, either immediately or after a preincubation step, onto a column conjugated with H4K20me1 peptides (outlined in the left panels of Figures 4D and 4E). His-3MBT protein bound to H4K20me1 in the presence of H1K26me3 peptides, but binding was completely inhibited by the presence of the H1K26me2 peptide (Figures 4D and 4E, right panels). This suggests that H1K26me2 and H4K20me1 bind to the same pocket within the three MBT domains. Interestingly, if equimolar amounts of H4K20me1 peptide were mixed with His-3MBT, competition was not complete, and a fraction of His-3MBT still bound to the H4K20me1 peptide column (Figure 4D, see lanes 2 and 3).

We next examined if the molecular basis of L3MBTL1-mediated chromatin compaction involves simultaneous binding to more than one nucleosome. A linearized DNA template containing nucleosome-positioning sequences exclusively at the 5′- and 3′-ends was generated. Native octamers were added to cover both nucleosome-positioning regions at the DNA ends, leaving the intervening DNA relatively naked (see Experimental Procedures). This chromatin template is suitable to screen for intra- and

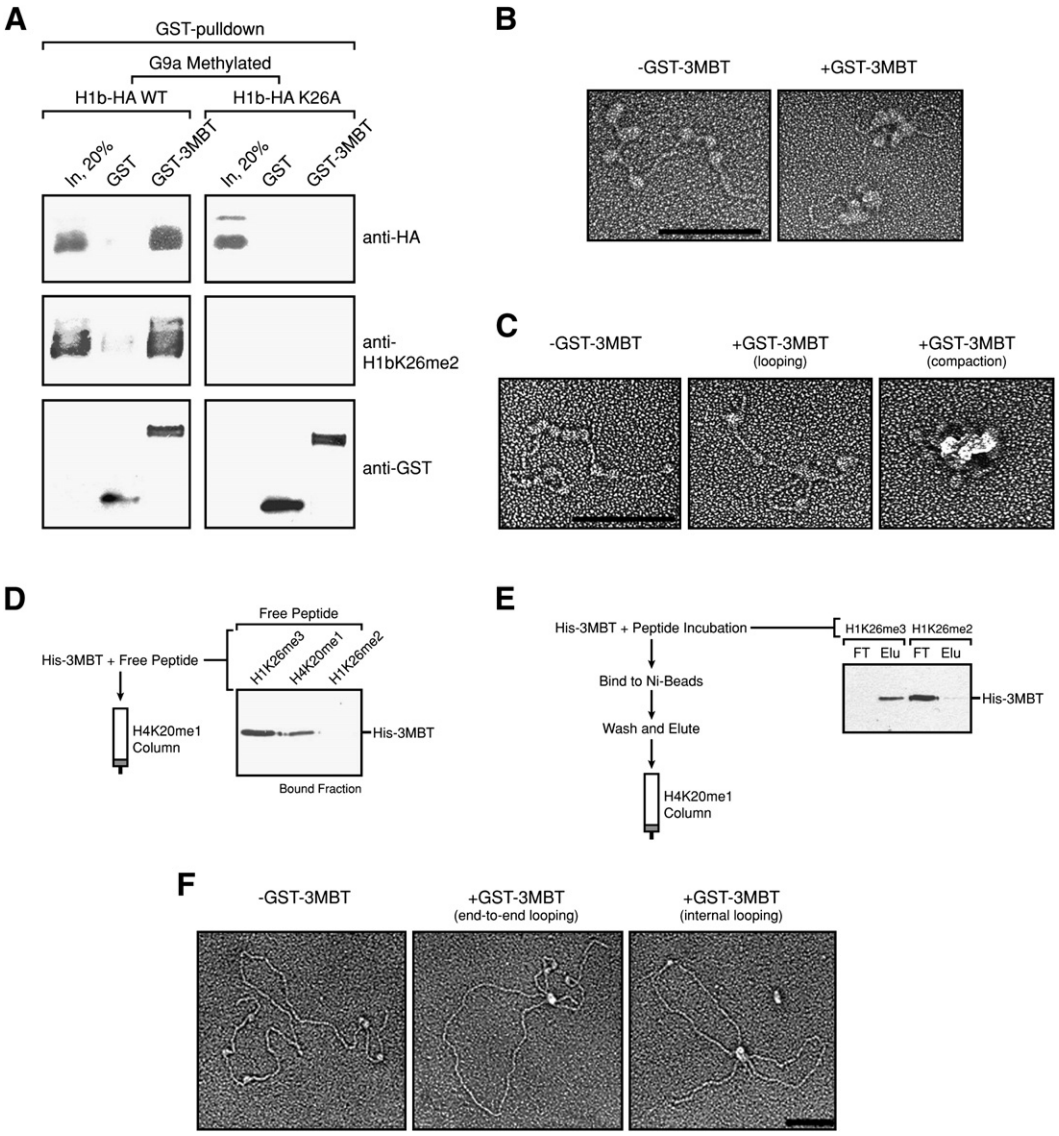

Figure 4. Reconstituted Nucleosomal Arrays with H1 Methylated at K26 Are Compacted by L3MBTL1

(A) GST pull-downs using GST or GST-3MBT with wild-type H1b or H1bK26A mutant protein premethylated by G9a analyzed by western blots.

(B) EM analysis shows that L3MBTL1 can compact recombinant reconstituted nucleosomal arrays with incorporated native H1. Scale bar is 100 nm.

(C) EM analysis shows that GST-3MBT caused looping and compaction of recombinant reconstituted nucleosomal arrays with G9a-methylated recombinant H1b incorporated. Scale bar is 100 nm.

(D) Left panel: schematic of competition assay. His-3MBT protein was added to a column containing H4K20me1 peptides covalently conjugated to agarose resin together with various free peptides (indicated in the right panel). Protein-peptide complexes were washed and eluted using 0.1 M glycine, pH 3.0. Right panel: western blot probed with anti-His antibody detecting the fraction retained on the H4K20me1 column. Free peptides are indicated above.

(E) Left panel: schematic of competition assay. His-3MBT protein was preincubated with either free H1K26me3 or H1K26me2 peptides, and the peptide-protein complex was prepurified with nickel resin. Eluted His-3MBT-peptide complexes were added to a column containing H4K20me1 peptides covalently conjugated to agarose resin. Protein-peptide complexes were washed and eluted using 0.1 M glycine, pH 3.0. Right panel: western blot probed with anti-His antibody detecting the fraction retained on the H4K20me1 column. Free peptides are indicated above.

(F) EM analysis shows that addition of GST-3MBT results in internal looping or end-to-end looping of native nucleosomal arrays. Scale bar is 100 nm.

internucleosome binding, which in the latter case would cause looping of the intervening DNA. Binding of GST-3MBT or His-3MBT to this chromatin template was confirmed by sucrose gradient sedimentation (data not shown), and fractions were examined by EM. As expected, nucleosomes were positioned at the DNA ends, and the intervening DNA was predominantly naked. The presence of GST-3MBT induced significant looping of

Table 1. Quantification of Chromatin Compaction/Looping Experiments

Type of Assay	Proteins Incubated with Nucleosomal Arrays			Total Molecules Analyzed	Looping and Compaction (%)
Compaction	nH1	− GST-3MBT		800	21.0
		+ GST-3MBT		900	45.0
	rH1b/G9a	− SAM	− GST-3MBT	400	15.5
			+ GST-3MBT	400	15.0
		+ SAM	− GST-3MBT	400	14.75
			+ GST-3MBT	400	32.75
	PR-SET7	− SAM	− GST-3MBT	500	12.8
			+ GST-3MBT	500	13.4
		+ SAM	− GST-3MBT	600	14.2
			+ GST-3MBT	400	39.75
			− His-3MBT	**600**	**15.8**
			+ His-3MBT (WT)	**600**	**50.8**
			+ His-3MBT (P2a)	**600**	**26.1**
			+ His-3MBT (P2b)	**600**	**33.3**
Looping	− GST-3MBT			1000	4.6
	+ GST-3MBT			1000	35.6
	+ GST-3MBT (P2)			400	15.75
	+ GST-3MBT (P1, P2, P3)			400	6.5
	+ His-3MBT-C2HC			500	35.2
	+ His-3MBT			500	17.8

Compaction assays have been performed using recombinant reconstituted nucleosomes, and looping assays have been performed with native nucleosomal arrays (subsaturating amounts of octamers). Percentage of compacted chromatin particles or particles showing looping upon addition of recombinant MBT domains in comparison to total number of analyzed particles is shown. The chromatin-compaction experiments carried out with monomeric His-3MBT protein are indicated in bold. All compaction assays have been carried out three to four times, and the looping assays (− GST-3MBT, + GST-3MBT) have been carried out four times or two times (all other looping experiments).

the DNA template with both nucleosomal regions being brought in close vicinity to each other (Figure 4F; see Table 1 for quantification). His-3MBT did induce looping but did so to a lesser extent than GST-3MBT (Figure S7; Table 1). To analyze the putative contribution of the Zn-finger domain of L3MBTL1 in looping, we generated a protein that is comprised of the three MBT domains and the Zn-finger domain (His-3MBT-C2HC; see Figure 1A). His-3MBT-C2HC protein migrated as a monomer in size-exclusion chromatography (Figure S1) but behaved in the looping assay similarly to the GST-3MBT protein (Figure S1; Table 1). Looping was reduced in the presence of the GST-3MBT-P2 mutant protein and completely abolished in the case of the triply mutated GST-3MBT protein (single point mutation in each of the three MBT domains; Table 1). Collectively, the results indicate that a monomeric form of L3MBTL1 allows internucleosome binding but that the C2HC domain or dimerization (via the SPM domain of the native protein or GST of the bacterially produced protein) contributes to this process (Table 1).

If monomeric His-3MBT is able to bind two nucleosomes simultaneously (Figure S7), then a single molecule might accommodate two methylated histone lysine residues. We tested this using our chromatin-compaction assay. Recombinant chromatin was monomethylated at H4K20 by PR-SET7, incubated with His-3MBT, and fractionated by sucrose gradient sedimentation (data not shown). The fractions analyzed by EM confirmed that His-3MBT indeed compacted chromatin solely dependent on a single histone lysine methylation mark, H4K20me1 (Figure S8; Table 1). However, if we used mutant His-3MBT containing a single amino acid substitution in the second MBT domain that is completely defective in binding to H4K20me1 (P2a), the number of compacted molecules decreased substantially (Figure S8; Table 1). A mutation in the second pocket that still exhibited binding to H4K20me1 (P2b) showed a reduced number of compacted particles compared to wild-type His-3MBT, but significantly more compared to the P2a mutant (Table 1).

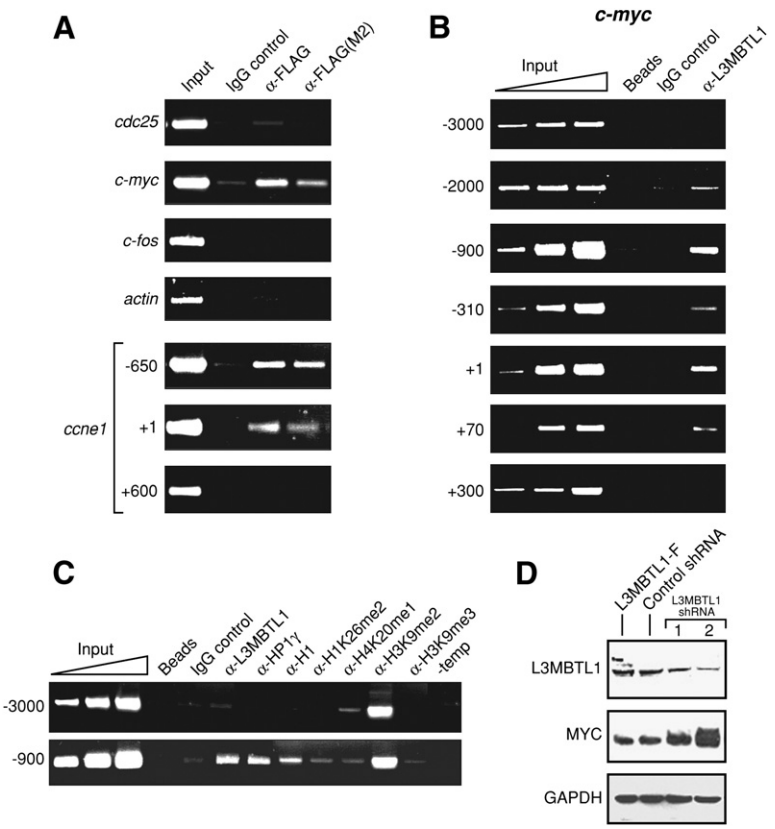

Figure 5. ChIP Experiments Identify L3MBTL1 Target Genes

(A) 293 cells stably expressing L3MBTL1-F in ChIP experiments using anti-FLAG mono- (M2) and polyclonal antibodies. Screening of E2F target genes revealed that L3MBTL1-F occupies *c-myc* and *ccne1* promoter regions. For *cdc25*, *c-myc*, *c-fos*, and *actin* genes a region around the transcriptional start site (+1) was analyzed, and for *cyclin E1 (ccne1)* the regions indicated were analyzed.

(B) HeLa cells were used for ChIP experiments to screen for the presence of endogenous L3MBTL1 on the *c-myc* promoter region.

(C) The −900 promoter region upstream of the *c-myc* transcriptional start site is occupied by L3MBTL1, H1, HP1γ, H4K20me1, H3K9me2, and H1K26me2. The −3000 region is not occupied by L3MBTL1, but H3K9me2 and H4K20me1 are present.

(D) ShRNA mediated decrease in L3MBTL1 protein levels. Lentiviral based stable knockdown of L3MBTL1 using two different *l3mbtl1* shRNA sequences (1 and 2) leads to increased MYC protein levels as analyzed by immunoblotting of nuclear extracts. A 293 cell line stably expressing ectopic L3MBTL1 (L3MBTL1-F) and a 293 cell line transduced with shRNA against an unrelated protein (Control shRNA) are also analyzed.

L3MBTL1 Occupies E2F Target Genes Together with HP1γ

Rb controls cell-cycle progression by binding to members of the E2F family of transcription factors to prevent gene activation. Since Rb copurified with L3MBTL1 (see Figure 1A) and the Drosophila L3MBTL1-homolog copurifies with a E2F/RBF complex (Lewis et al., 2004), we tested if L3MBTL1 also localizes to E2F-regulated genes such as *c-myc* and *cyclin E1* (*ccne1*). Chromatin immunoprecipitation (ChIP) experiments using 293 cells stably expressing L3MBTL1-F demonstrated binding of L3MBTL1-F to the proximal promoter regions of *c-myc* and *ccne1* genes (Figure 5A). L3MBTL1-F was not detectable downstream of the transcription start site of the *cyclin E* gene, nor at the *cdc25*, *c-fos*, and *actin* promoters (Figure 5A), demonstrating specificity of the assay.

To explore chromatin binding of the endogenous L3MBTL1 protein, we generated a specific anti-L3MBTL1 antibody (Figure S9). ChIP experiments confirmed binding of endogenous L3MBTL1 to the *c-myc* gene (Figure 5B). The biochemical experiments (see above) strongly suggested that H4K20me1 and H1K26me1/2 should be present at these genes, and we found this to be the case for *c-myc* using ChIP assays (Figure 5C). Importantly, within the *c-myc* promoter region (−900 bp from the transcriptional start site, TSS) the presence of H1bK26me1/2, HP1γ, and H4K20me1 correlates well with the presence of L3MBTL1. Interestingly, H3K9me2 but not H3K9me3 was also present at these regions of the *c-myc* gene. H3K9me2 likely serves as a site for HP1γ binding. Sequences upstream (−3000) or downstream of the TSS were devoid of L3MBTL1, H1b, or HP1γ (Figures 5B and 5C; data not shown).

Our results suggest that L3MBTL1 functions as a transcriptional repressor, at least in part, by compacting chromatin. To analyze further whether L3MBTL1 impacts *c-myc* gene expression, we used RNA interference. Short hairpin RNAs (shRNA) against *l3mbtl1* led to a decrease in L3MBTL1 protein levels concomitant with a significant increase in MYC protein levels (Figure 5D). These results are consistent with our model that L3MBTL1 negatively regulates *c-myc* gene expression. This is also consistent with the finding that Drosophila L(3)MBT functions in transcriptional repression (Lewis et al., 2004).

DISCUSSION

A Novel Facet of Facultative Chromatin Compaction

The transcriptional repressor L3MBTL1 compacts chromatin in a manner that is strictly dependent on histone methylation marks—specifically H4K20me1/2 and H1K26me1/2 as shown in this report. The apparent exclusivity of L3MBTL1 for mono- and dimethylated states supports a model in which different degrees of methylation at a particular site can give rise to different readouts. The chromodomains (Fischle et al., 2003; Flanagan et al., 2005; Sims

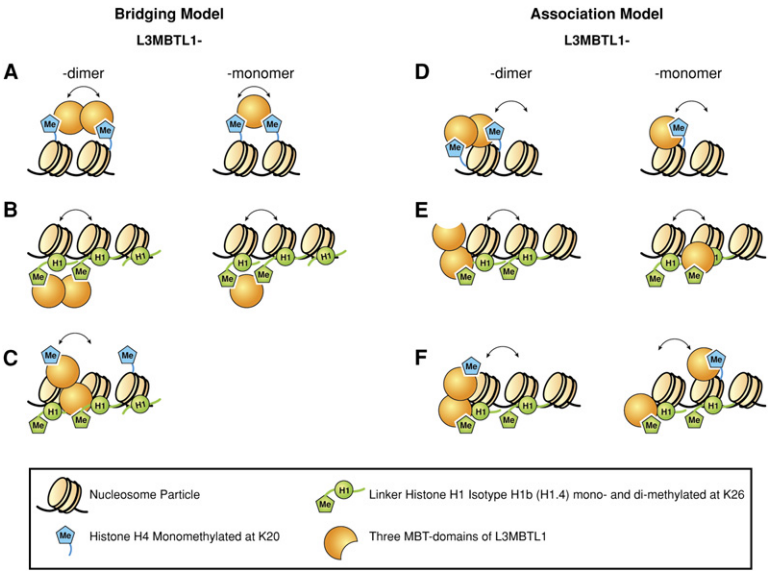

Figure 6. Alternate Models for L3MBTL1 Compaction of Nucleosomal Arrays

See text for details.

Bridging model. One L3MBTL1 monomer or dimer binds to two nucleosomes moving them into close vicinity. In the monomeric case, one molecule containing three MBT repeats can accommodate either: (A) two H4K20me1 or (B) two H1K26me1/2 marks on the histone tails of adjacent nucleosomes or chromatosomes, respectively. For simplicity, in the L3MBTL1-homodimer case only one of two marks bound by each monomer is illustrated. The homodimer could accommodate four of one type of mark, (A) H4K20me1 or (B) H1K26me1/2, or it could accommodate (C) two of each type on adjacent nucleosomes.

Association model: Each homodimeric or monomeric L3MBTL1 binds one nucleosome and facilitates linker DNA bending or internucleosomal interactions. As shown in the monomeric case, L3MBTL1 molecules would be positioned on (D) the surface of the nucleosome or (E) the chromatosome by specific binding to either H4K20me1 or H1K26me1/2, respectively, leading to a compacted chromatin state. The same is true for the L3MBTL1 homodimer except that (F) both marks could be accommodated.

et al., 2005) and PHD-domains (Shi et al., 2006; Wysocka et al., 2006; Li et al., 2006; Pena et al., 2006) found in several proteins provide a paradigm for this model, given their preference for di- and trimethylated lysines as compared to the monomethyl state.

The binding specificities of L3MBTL1 raise an important question. How do the MBT repeats bind specifically to two different methylated lysine residues (H4K20me1/2 and H1K26me1/2)? Even more intriguing is that the MBT domains bind H1K26me1/2 but not H3K9me2/3 or H3K27me1/2/3, yet these lysine residues are located within a conserved consensus sequence (ARKS). The simplest explanation would be that each one of the three MBT domains binds a different ligand. However, our data and that of others (Kim et al., 2006) suggest otherwise. The second MBT domain is important for H1K26me1/2 as well as for H4K20me1/2 binding (Figure 3F), as pre binding with H1K26me2 peptides abolished 3MBT binding to H4K20me1 (Figures 4D and 4E). Moreover, since we identified a mutant in the second MBT domain that abolishes binding to both ligands and a second mutant that selectively abolishes H1K26me, but not H4K20me, binding, we suggest that both methylated residues are bound via the second MBT domain but that different aromatic residues are involved in caging the methylated lysine residue. Caging through aromatic residues is a property of all proteins that specifically recognize methylated lysine residues (Flanagan et al., 2005; Huang et al., 2006; Jacobs and Khorasanizadeh, 2002; Li et al., 2006; Nielsen et al., 2002; Pena et al., 2006).

With respect to chromatin compaction, we envision two different scenarios, taking into account that the P2 domain of L3MBTL1 can bind H4K20me1 or H1K26me1/2 but apparently not both modifications simultaneously. Importantly, monomeric 3MBT can still compact chromatin in our assay conditions, suggesting that the P2 domain can accommodate two modified histone marks on two nucleosomes. However, given that pre binding with H1K26me2 peptides abolished 3MBT binding to H4K20me1, the two marks accommodated by the monomer must be identical. Thus, in the case of the dimeric L3MBTL1, each of the monomers would bind two identical marks such that four H4K20me1, four H1K26me1/2, or two of each mark are bound.

In the ''bridging model'' L3MBTL1 functions either as a monomer or a dimer, and adjacent nucleosomes or chromatosomes are bound simultaneously, thereby bridging the linker DNA and moving the nucleosomes closer together (Figure 6A). L3MBTL1 does exist as a homodimer in vivo (Boccuni et al., 2003), and dimerization is one mechanism by which two L3MBTL1 molecules bind to H4K20me1 and H1K26me1/2 on adjacent nucleosomes/chromatosomes. This is also supported by our looping experiments (Figures 4F and S7). Yet, repression does not depend on the SPM domain responsible for L3MBTL1 homodimerization, and a monomeric 3MBT molecule lacking the SPM domain still shows compaction in our assays (Figures S2 and S7) and can repress transcription when directed to a reporter (Boccuni et al., 2003). Nonetheless, chromatin compaction by a single 3MBT molecule is still consistent with the bridging model. A similar mechanism for binding and compacting of multiple nucleosomes by a single molecule was reported recently in the case of the PRC1 component PSC (Francis

et al., 2004), but the histone tails or histone lysine methylation marks were not required. In this case, the compacted particles resembled the chromatin structures that we observed in the presence of L3MBTL1.

In the "association model" a single L3MBTL1 molecule (monomer or dimer) could compact chromatin by positioning itself on the surface of the nucleosome/chromatosome in a fashion that promotes bending of the linker DNA or facilitates histone-histone interactions (Figure 6B). In this model, correct positioning of L3MBTL1 is accomplished by the specific recognition of H4K20me1 or H1K26me1/2 on the nucleosome or chromatosome surface, respectively. The linker histone itself functions in a similar manner (Wollfe, 1998). Moreover, proteins containing HMG boxes, the transcription factor HNF3, the myeloid and erythroid nuclear termination stage-specific protein (MENT; Springhetti et al., 2003), or PARP-1 (Kim et al., 2004) can also bind to nucleosomes and alter chromatin conformation. In the case of L3MBTL1, compaction is dependent on specific methylated lysine residues adding a distinct regulatory parameter.

Concerted Actions of Histone H1b and L3MBTL1 during Chromatin Compaction

Linker histone H1 functions as a transcriptional repressor in vitro (Cheung et al., 2002; Croston et al., 1991; Laybourn and Kadonaga, 1991) and is important in chromatin folding in vitro (van Holde, 1989; Wolffe, 1997). The C-terminal region of H1 is required for its binding to DNA between nucleosomes (Bednar et al., 1998), and H1 phosphorylation changes its ability to bind to chromatin (Dou et al., 1999). Here we show that L3MBTL1 interacts with H1 in a methylation-dependent manner and that H1bK26me1/2 is important for chromatin compaction by the MBT domains (Figure 4C). H1 has been detected on both transcriptionally active and inactive genes (reviewed by Parseghian and Hamkalo, 2001), and its binding to chromatin is dynamic in vivo (Lever et al., 2000; Misteli et al., 2000), yet the number of factors affecting H1 mobility is unknown (discussed in van Holde and Zlatanova, 2006). It is possible that methylation of histone H1 at lysine-26 in the presence of L3MBTL1 increases H1 residence time on chromatin, thereby facilitating a compacted chromatin state.

MBT Domain Proteins and Gene Expression

The specificity of the proteins involved in establishing a type of facultative heterochromatin is likely dictated by the interaction of regulators (E2F) with other regulators (Rb) and factors that function in compacting chromatin. L3MBTL1 is a member of a large family of mammalian MBT proteins that contain variable numbers of MBT domains. These domains are not identical in sequence, as is also the case with the chromo- and bromo-domains. Given this, the different members of the MBT family might recognize different patterns of histone methyl marks to establish repression of specific genes through the formation of facultative heterochromatin.

One of the L3MBTL1 targets shown here is *c-myc*, the expression of which is tightly regulated, with increased myc expression often correlated with cancer (for review see Nilsson and Cleveland, 2003). We found that reduction of L3MBTL1 levels significantly increases MYC protein levels. Ectopic expression of L3MBTL1, however, does not affect MYC protein levels (Figure 5D). This is perhaps not surprising given that our in vitro data show a specific requirement for histone methylation marks in binding; thus, increased expression of L3MBTL1 would not necessarily lead to its increased chromatin binding. It remains to be investigated if overexpression of *myc* in cancer correlates with aberrant *L3mbtl1* gene expression and/or localization. The human L3MBTL1 gene is located on chromosome 20q within the region commonly deleted in patients with myeloproliferative disorders (MacGrogan et al., 2001). It is also possible that the chromatin signature (e.g., histone methylation marks) of the *c-myc* promoter region is abnormal in malignant cells, thereby altering L3MBTL1 binding and the regulated expression of *c-myc*.

EXPERIMENTAL PROCEDURES

Biochemical Purification of L3MBTL1-F and Associated Polypeptides

Full-length *l3mbtl1* cDNA was inserted into pCMV-Tag4A and transfected in 293 cells using FuGENE (Roche), and clones were selected that stably expressed the L3MBTL1-FLAG fusion protein. Nuclear extracts (~300 mg) were prepared from 45 liters of culture following the Dignam protocol (Dignam et al., 1983) and subjected to anti-FLAG (M2) agarose (Sigma). Bound proteins were eluted with 200 μg/ml FLAG peptide (Sigma). Affinity-purified L3MBTL1-F fractions were resolved by SDS-PAGE and analyzed by silver staining, western blotting, and mass spectrometry. Gel-resolved proteins were digested with trypsin, the mixtures fractionated on a Poros 50 R2 RP microtip, and the resulting peptide pools analyzed by matrix-assisted laser-desorption/ionization reflectron time-of-flight (MALDI-reTOF) MS using a BRUKER UltraFlex TOF/TOF instrument (Bruker; Bremen, Germany) as described (Devroe et al., 2004).

Peptide Affinity Chromatography

Peptide-affinity columns were generated using SulfoLink coupling gel (Pierce). Histone H1b peptides comprised residues 20–37 with K26 either unmodified, mono-, di-, or trimethylated. Additional peptides include H3K4 (residues 1–8), H3K9 (residues 5–13), H3K27 (20–33), and H4K20 (residues 16–25). Peptide-bound proteins (either in-vitro-translated or 10 ug of recombinant protein) were washed extensively (60 column volumes of 25 mM Tris, pH 8, 150 mM NaCl, 2 mM EDTA, and 0.5% NP40) and eluted with either 0.5 mg/ml peptide or low pH buffer (100 mM glycine, pH 3.0; Sims et al., 2006).

Chromatin-Compaction Assay

Two micrograms of nucleosome arrays were reconstituted as previously described (Nishioka and Reinberg, 2003) and incubated with recombinant 3MBT proteins in HE buffer containing 25 mM KCl at a molar ratio of 1:4 at RT for 60 min. The protein-nucleosome complexes were loaded onto a 5%–30% sucrose gradient in HE buffer containing 25 mM KCl and centrifugated for 6.5–15 hr at 25,000 RPM, and the fractions were analyzed by 1.0% agarose gel electrophoresis. Peak fractions of the protein-nucleosome complexes were analyzed by EM.

EM

Protein-nucleosome complexes were fixed with 0.6% glutaraldehyde, and DNA-protein complexes were purified by gravity-flow gel filtration (2 ml of BIO-GEL A-5M resin or Sepharose CL-4B, BioRad) using TE buffer. Purified protein-nucleosome complexes were mixed with a buffer containing spermidine to a final concentration of 2 mM, adsorbed to glow-charged carbon-coated grids, washed with a water/graded ethanol series, and rotary shadow cast with tungsten (Griffith and Christiansen, 1978). Samples were examined using a JEOL 1200 EX transmission electron microscope. Micrographs are shown in reverse contrast. A Cohu CCD camera attached to a Macintosh computer programmed with National Institute of Health (NIH) IMAGE software was used to prepare the images.

ChIP and RNAi

ChIP assays were performed as described (Lewis et al., 2005; Vaquero et al., 2004). ChIP samples were prepared from 293 cells stably expressing L3MBTL1-F and from HeLa cells. Primer sets were chosen to amplify approximately 200 bp around the indicated region. Primer sequences are available upon request. Five different *l3mbtl1* short hairpin (sh) RNA constructs were obtained from the MISSION TRC-Hs 1.0 (Human) shRNA library (SIGMA) and used as described previously (Zufferey et al., 1998).

Supplemental Data

Supplemental Data include nine figures and can be found with this article online at http://www.cell.com/cgi/content/full/129/5/915/DC1/.

ACKNOWLEDGMENTS

We are grateful to Dr. Lynne Vales for critical reading of our manuscript and for helpful comments. We thank Drs. Pierre Chambon and Regine Losson for the generous gift of antibodies. This work is supported by an Erwin Schrödinger Fellowship from the Austrian Science Foundation (FWF) to P.T. (J2354-B12), a NIH postdoctoral fellowship to R.J.S. (GM-71166), and by grants from the National Institutes of Health (CA085826 and CA113863 to Y.-H.W., CA 102202 to S.D.N., and GM-64844 to D.R.) and the Howard Hughes Medical Institute to D.R.

Received: July 24, 2006
Revised: December 27, 2006
Accepted: March 12, 2007
Published: May 31, 2007

REFERENCES

Bannister, A.J., Zegerman, P., Partridge, J.F., Miska, E.A., Thomas, J.O., Allshire, R.C., and Kouzarides, T. (2001). Selective recognition of methylated lysine 9 on histone H3 by the HP1 chromo domain. Nature *410*, 120–124.

Bednar, J., Horowitz, R.A., Dubochet, J., and Woodcock, C.L. (1995). Chromatin conformation and salt-induced compaction: three-dimensional structural information from cryoelectron microscopy. J. Cell Biol. *131*, 1365–1376.

Bednar, J., Horowitz, R.A., Grigoryev, S.A., Carruthers, L.M., Hansen, J.C., Koster, A.J., and Woodcock, C.L. (1998). Nucleosomes, linker DNA, and linker histone form a unique structural motif that directs the higher-order folding and compaction of chromatin. Proc. Natl. Acad. Sci. USA *95*, 14173–14178.

Boccuni, P., MacGrogan, D., Scandura, J.M., and Nimer, S.D. (2003). The human L(3)MBT polycomb group protein is a transcriptional repressor and interacts physically and functionally with TEL (ETV6). J. Biol. Chem. *278*, 15412–15420.

Cheung, E., Zarifyan, A.S., and Kraus, W.L. (2002). Histone H1 represses estrogen receptor alpha transcriptional activity by selectively inhibiting receptor-mediated transcription initiation. Mol. Cell. Biol. *22*, 2463–2471.

Croston, G.E., Kerrigan, L.A., Lira, L.M., Marshak, D.R., and Kadonaga, J.T. (1991). Sequence-specific antirepression of histone H1-mediated inhibition of basal RNA polymerase II transcription. Science *251*, 643–649.

Daujat, S., Zeissler, U., Waldmann, T., Happel, N., and Schneider, R. (2005). HP1 binds specifically to Lys26-methylated histone H1.4, whereas simultaneous Ser27 phosphorylation blocks HP1 binding. J. Biol. Chem. *280*, 38090–38095.

Devroe, E., Erdjument-Bromage, H., Tempst, P., and Silver, P.A. (2004). Human Mob proteins regulate the NDR1 and NDR2 serine-threonine kinases. J. Biol. Chem. *279*, 24444–24451.

Dignam, J.D., Lebovitz, R.M., and Roeder, R.G. (1983). Accurate transcription initiation by RNA polymerase II in a soluble extract from isolated mammalian nuclei. Nucleic Acids Res. *11*, 1475–1489.

Dou, Y., Mizzen, C.A., Abrams, M., Allis, C.D., and Gorovsky, M.A. (1999). Phosphorylation of linker histone H1 regulates gene expression in vivo by mimicking H1 removal. Mol. Cell *4*, 641–647.

Fischle, W., Wang, Y., Jacobs, S.A., Kim, Y., Allis, C.D., and Khorasanizadeh, S. (2003). Molecular basis for the discrimination of repressive methyl-lysine marks in histone H3 by Polycomb and HP1 chromodomains. Genes Dev. *17*, 1870–1881.

Flanagan, J.F., Mi, L.Z., Chruszcz, M., Cymborowski, M., Clines, K.L., Kim, Y., Minor, W., Rastinejad, F., and Khorasanizadeh, S. (2005). Double chromodomains cooperate to recognize the methylated histone H3 tail. Nature *438*, 1181–1185.

Francis, N.J., Kingston, R.E., and Woodcock, C.L. (2004). Chromatin compaction by a polycomb group protein complex. Science *306*, 1574–1577.

Griffith, J.D., and Christiansen, G. (1978). Electron microscope visualization of chromatin and other DNA-protein complexes. Annu. Rev. Biophys. Bioeng. *7*, 19–35.

Hall, I.M., Shankaranarayana, G.D., Noma, K., Ayoub, N., Cohen, A., and Grewal, S.I. (2002). Establishment and maintenance of a heterochromatin domain. Science *297*, 2232–2237.

Huang, Y., Fang, J., Bedford, M.T., Zhang, Y., and Xu, R.M. (2006). Recognition of histone H3 lysine-4 methylation by the double tudor domain of JMJD2A. Science *312*, 748–751.

Jacobs, S.A., and Khorasanizadeh, S. (2002). Structure of HP1 chromodomain bound to a lysine 9-methylated histone H3 tail. Science *295*, 2080–2083.

Jacobs, S.A., Taverna, S.D., Zhang, Y., Briggs, S.D., Li, J., Eissenberg, J.C., Allis, C.D., and Khorasanizadeh, S. (2001). Specificity of the HP1 chromo domain for the methylated N-terminus of histone H3. EMBO J. *20*, 5232–5241.

Kim, J., Daniel, J., Espejo, A., Lake, A., Krishna, M., Xia, L., Zhang, Y., and Bedford, M.T. (2006). Tudor, MBT and chromo domains gauge the degree of lysine methylation. EMBO Rep. *4*, 397–403.

Kim, M.Y., Mauro, S., Gevry, N., Lis, J.T., and Kraus, W.L. (2004). NAD+-dependent modulation of chromatin structure and transcription by nucleosome binding properties of PARP-1. Cell *119*, 803–814.

Klymenko, T., Papp, B., Fischle, W., Kocher, T., Schelder, M., Fritsch, C., Wild, B., Wilm, M., and Muller, J. (2006). A Polycomb group protein complex with sequence-specific DNA-binding and selective methyl-lysine-binding activities. Genes Dev. *20*, 1110–1122.

Kuzmichev, A., Jenuwein, T., Tempst, P., and Reinberg, D. (2004). Different EZH2-containing complexes target methylation of histone H1 or nucleosomal histone H3. Mol. Cell *14*, 183–193.

Kuzmichev, A., Margueron, R., Vaquero, A., Preissner, T.S., Scher, M., Kirmizis, A., Ouyang, X., Brockdorff, N., Abate-Shen, C., Farnham, P., and Reinberg, D. (2005). Composition and histone substrates of

polycomb repressive group complexes change during cellular differentiation. Proc. Natl. Acad. Sci. USA *102*, 1859–1864.

Laybourn, P.J., and Kadonaga, J.T. (1991). Role of nucleosomal cores and histone H1 in regulation of transcription by RNA polymerase II. Science *254*, 238–245.

Lever, M.A., Th'ng, J.P., Sun, X., and Hendzel, M.J. (2000). Rapid exchange of histone H1.1 on chromatin in living human cells. Nature *408*, 873–876.

Lewis, B.A., Sims, R.J., 3rd, Lane, W.S., and Reinberg, D. (2005). Functional characterization of core promoter elements: DPE-specific transcription requires the protein kinase CK2 and the PC4 coactivator. Mol. Cell *18*, 471–481.

Lewis, P.W., Beall, E.L., Fleischer, T.C., Georlette, D., Link, A.J., and Botchan, M.R. (2004). Identification of a Drosophila Myb-E2F2/RBF transcriptional repressor complex. Genes Dev. *18*, 2929–2940.

Li, H., Ilin, S., Wang, W., Duncan, E.M., Wysocka, J., Allis, C.D., and Patel, D.J. (2006). Molecular basis for site-specific read-out of histone H3K4me3 by the BPTF PHD finger of NURF. Nature *442*, 91–95.

Loyola, A., LeRoy, G., Wang, Y.H., and Reinberg, D. (2001). Reconstitution of recombinant chromatin establishes a requirement for histone-tail modifications during chromatin assembly and transcription. Genes Dev. *15*, 2837–2851.

MacGrogan, D., Alvarez, S., DeBlasio, T., Jhanwar, S.C., and Nimer, S.D. (2001). Identification of candidate genes on chromosome band 20q12 by physical mapping of translocation breakpoints found in myeloid leukemia cell lines. Oncogene *20*, 4150–4160.

Maison, C., Bailly, D., Peters, A.H., Quivy, J.P., Roche, D., Taddei, A., Lachner, M., Jenuwein, T., and Almouzni, G. (2002). Higher-order structure in pericentric heterochromatin involves a distinct pattern of histone modification and an RNA component. Nat. Genet. *30*, 329–334.

Meehan, R.R., Kao, C.F., and Pennings, S. (2003). HP1 binding to native chromatin in vitro is determined by the hinge region and not by the chromodomain. EMBO J. *22*, 3164–3174.

Minc, E., Courvalin, J.C., and Buendia, B. (2000). HP1gamma associates with euchromatin and heterochromatin in mammalian nuclei and chromosomes. Cytogenet. Cell Genet. *90*, 279–284.

Misteli, T., Gunjan, A., Hock, R., Bustin, M., and Brown, D.T. (2000). Dynamic binding of histone H1 to chromatin in living cells. Nature *408*, 877–881.

Nielsen, P.R., Nietlispach, D., Mott, H.R., Callaghan, J., Bannister, A., Kouzarides, T., Murzin, A.G., Murzina, N.V., and Laue, E.D. (2002). Structure of the HP1 chromodomain bound to histone H3 methylated at lysine 9. Nature *416*, 103–107.

Nielsen, S.J., Schneider, R., Bauer, U.M., Bannister, A.J., Morrison, A., O'Carroll, D., Firestein, R., Cleary, M., Jenuwein, T., Herrera, R.E., and Kouzarides, T. (2001). Rb targets histone H3 methylation and HP1 to promoters. Nature *412*, 561–565.

Nilsson, J.A., and Cleveland, J.L. (2003). Myc pathways provoking cell suicide and cancer. Oncogene *22*, 9007–9021.

Nishioka, K., and Reinberg, D. (2003). Methods and tips for the purification of human histone methyltransferases. Methods *31*, 49–58.

Nishioka, K., Rice, J.C., Sarma, K., Erdjument-Bromage, H., Werner, J., Wang, Y., Chuikov, S., Valenzuela, P., Tempst, P., Steward, R., et al. (2002). PR-Set7 is a nucleosome-specific methyltransferase that modifies lysine 20 of histone H4 and is associated with silent chromatin. Mol. Cell *9*, 1201–1213.

Ogawa, H., Ishiguro, K., Gaubatz, S., Livingston, D.M., and Nakatani, Y. (2002). A complex with chromatin modifiers that occupies E2F- and Myc-responsive genes in G0 cells. Science *296*, 1132–1136.

Parseghian, M.H., and Hamkalo, B.A. (2001). A compendium of the histone H1 family of somatic subtypes: an elusive cast of characters and their characteristics. Biochem. Cell Biol. *79*, 289–304.

Patnaik, D., Chin, H.G., Esteve, P.O., Benner, J., Jacobsen, S.E., and Pradhan, S. (2004). Substrate specificity and kinetic mechanism of mammalian G9a histone H3 methyltransferase. J. Biol. Chem. *279*, 53248–53258.

Pena, P.V., Davrazou, F., Shi, X., Walter, K.L., Verkhusha, V.V., Gozani, O., Zhao, R., and Kutateladze, T.G. (2006). Molecular mechanism of histone H3K4me3 recognition by plant homeodomain of ING2. Nature *442*, 100–103.

Sato, M.H., Ura, K., Hohmura, K.I., Tokumasu, F., Yoshimura, S.H., Hanaoka, F., and Takeyasu, K. (1999). Atomic force microscopy sees nucleosome positioning and histone H1-induced compaction in reconstituted chromatin. FEBS Lett. *452*, 267–271.

Schotta, G., Ebert, A., Krauss, V., Fischer, A., Hoffmann, J., Rea, S., Jenuwein, T., Dorn, R., and Reuter, G. (2002). Central role of Drosophila SU(VAR)3–9 in histone H3–K9 methylation and heterochromatic gene silencing. EMBO J. *21*, 1121–1131.

Shi, X., Hong, T., Walter, K.L., Ewalt, M., Michishita, E., Hung, T., Carney, D., Pena, P., Lan, F., Kaadige, M.R., et al. (2006). ING2 PHD domain links histone H3 lysine 4 methylation to active gene repression. Nature *442*, 96–99.

Sims, R.J., 3rd, Nishioka, K., and Reinberg, D. (2003). Histone lysine methylation: a signature for chromatin function. Trends Genet. *19*, 629–639.

Sims, R.J., 3rd, Chen, C.F., Santos-Rosa, H., Kouzarides, T., Patel, S.S., and Reinberg, D. (2005). Human but not yeast CHD1 binds directly and selectively to histone H3 methylated at lysine 4 via its tandem chromodomains. J. Biol. Chem. *280*, 41789–41792.

Sims, R.J., 3rd, Trojer, P., Li, G., and Reinberg, D. (2006). Methods to identify and functionally analyze factors that specifically recognize histone lysine methylation. Methods *40*, 331–338.

Springhetti, E.M., Istomina, N.E., Whisstock, J.C., Nikitina, T., Woodcock, C.L., and Grigoryev, S.A. (2003). Role of the M-loop and reactive center loop domains in the folding and bridging of nucleosome arrays by MENT. J. Biol. Chem. *278*, 43384–43393.

Tachibana, M., Sugimoto, K., Fukushima, T., and Shinkai, Y. (2001). Set domain-containing protein, G9a, is a novel lysine-preferring mammalian histone methyltransferase with hyperactivity and specific selectivity to lysines 9 and 27 of histone H3. J. Biol. Chem. *276*, 25309–25317.

van Holde, K., and Zlatanova, J. (2006). Scanning chromatin: a new paradigm? J. Biol. Chem. *281*, 12197–12200.

van Holde, K.E. (1989). Chromatin, *Volume 1*, First Edition, (New York: Springer-Verlag).

Vaquero, A., Scher, M., Lee, D., Erdjument-Bromage, H., Tempst, P., and Reinberg, D. (2004). Human SirT1 interacts with histone H1 and promotes formation of facultative heterochromatin. Mol. Cell *16*, 93–105.

Wang, W.K., Tereshko, V., Boccuni, P., MacGrogan, D., Nimer, S.D., and Patel, D.J. (2003). Malignant brain tumor repeats: a three-leaved propeller architecture with ligand/peptide binding pockets. Structure *11*, 775–789.

Wismar, J., Loffler, T., Habtemichael, N., Vef, O., Geissen, M., Zirwes, R., Altmeyer, W., Sass, H., and Gateff, E. (1995). The Drosophila melanogaster tumor suppressor gene lethal(3)malignant brain tumor encodes a proline-rich protein with a novel zinc finger. Mech. Dev. *53*, 141–154.

Wolffe, A.P. (1997). Histone H1. Int. J. Biochem. Cell Biol. *29*, 1463–1466.

Wollfe, A. (1998). Chromatin: Structure and Function (Wiltshire, Great Britain: Academic Press).

Wysocka, J., Swigut, T., Xiao, H., Milne, T.A., Kwon, S.Y., Landry, J., Kauer, M., Tackett, A.J., Chait, B.T., Badenhorst, P., et al. (2006). A PHD finger of NURF couples histone H3 lysine 4 trimethylation with chromatin remodelling. Nature *442*, 86–90.

Yohn, C.B., Pusateri, L., Barbosa, V., and Lehmann, R. (2003). l(3)malignant brain tumor and three novel genes are required for Drosophila germ-cell formation. Genetics *165*, 1889–1900.

Zhao, T., Heyduk, T., Allis, C.D., and Eissenberg, J.C. (2000). Heterochromatin protein 1 binds to nucleosomes and DNA in vitro. J. Biol. Chem. *275*, 28332–28338.

Zufferey, R., Dull, T., Mandel, R.J., Bukovsky, A., Quiroz, D., Naldini, L., and Trono, D. (1998). Self-inactivating lentivirus vector for safe and efficient in vivo gene delivery. J. Virol. *72*, 9873–9880.